

Solidification of Emulsified Polymer Solutions via Phase Inversion (SEMPI): A Generic Way To Prepare Polymers with Controlled Porosity

Pieter Vandezande,[†] Lieven E. M. Gevers,^{†,‡} Jan Vermant,[§] Johan A. Martens,[†]
Pierre A. Jacobs,[†] and Ivo F. J. Vankelecom^{*,†}

Centre for Surface Science and Catalysis, Department of Microbial and Molecular Systems, Katholieke Universiteit Leuven, Kasteelpark Arenberg 23-box 2461, B-3001 Leuven, Belgium, Applied Rheology and Polymer Processing Division, Department of Chemical Engineering, Katholieke Universiteit Leuven, Willem de Croylaan 46, B-3001 Leuven, Belgium

Received January 23, 2008. Revised Manuscript Received March 6, 2008

Porous polymeric structures with controlled porosity were prepared using a new approach involving solidification of emulsified polymer solutions via phase inversion (SEMPI). The new method starts from a polymeric emulsion for which the presence of nanosized particles or surfactants is crucial. Subsequent solidification of such emulsion is realized by simple contact with a polymer nonsolvent. The resulting solids exhibit spherical pores for which the emulsion droplets act as template. The preparation method allows easy control over pore morphology by tuning a number of easily accessible parameters, mainly at the level of the emulsion itself. A wide variety of polymers, including biocompatible and biodegradable polymers, can thus be turned into porous materials. Two typical applications in controlled release and solvent resistant nanofiltration are presented, illustrating the real practical utility of the presented method. Compared with the commonly used methods to prepare porous polymers, the presented method has a large potential since it (1) is applicable to a wide range of different polymers, (2) shows simply accessible flexibility in structural properties, such as porosity, pore size, pore interconnectivity, and pore wall functionality, (3) involves no chemical reaction in the polymer hardening process, and (4) allows creation of porous materials with an asymmetric structure.

1. Introduction

Over the past years, membrane separations have gained significant importance as an energy- and waste-efficient technique to separate all kinds of gaseous and liquid mixtures. Membranes can be either ceramic or polymeric in nature. Particularly attractive membrane materials are however created by mixing both types of materials, typically by dispersing an inorganic filler in a polymeric matrix. They are referred to as either mixed matrix, organomineral, hybrid, or composite membranes.^{1,2} The fillers mostly enhance the membrane properties directly through their specific adsorptive or diffusive properties. Indirectly, they can modify the membrane structure in such a way that a better membrane morphology is formed, leading for instance to enhanced compaction resistance³ or chemical stability.⁴ Among the most popular fillers are zeolites, carbon black, silica, and

metal oxides. These fillers have already been introduced in a variety of polymer types and tested in many membrane applications, such as gas separation,^{5,6} pervaporation,^{7,8} nanofiltration,^{4,9,10} ultrafiltration,^{11,12} and as membrane adsorber.¹³ Membranes used in nanofiltration, gas separation, and pervaporation need to discriminate between small molecules; hence, the selective layers are intrinsically quite dense and require submicron thicknesses to allow reasonable fluxes. One of the most popular ways to prepare membranes with thin selective top layers is via the process of phase inversion,^{14,15} in which a cast polymer solution is typically solidified upon emersion in a nonsolvent bath. For such

* Corresponding author. Tel.: (+32) 16-321594. Fax: (+32) 16-321998. E-mail: ivo.vankelecom@biw.kuleuven.be.

[†] Centre for Surface Science and Catalysis.

[‡] Current address: Umicore site Olen, Watertorenstraat 33, B-2250 Olen, Belgium.

[§] Applied Rheology and Polymer Processing Division.

(1) Chung, T. S.; Jiang, L. Y.; Li, Y.; Kulprathipanja, S. *Prog. Polym. Sci.* **2007**, *32*, 483.

(2) Moore, T. T.; Mahajan, R.; Vu, D. Q.; Koros, W. J. *AIChE J.* **2004**, *50*, 311.

(3) Nunes, S. P.; Peinemann, K. V.; Ohlrogge, K.; Alpers, A.; Keller, M.; Pires, A. T. N. *J. Membr. Sci.* **1999**, *157*, 219.

(4) Gevers, L. E. M.; Vankelecom, I. F. J.; Jacobs, P. A. *Chem. Commun.* **2005**, *19*, 2500.

(5) De Sitter, K.; Winberg, P.; D'Haen, J.; Dotremont, C.; Leysen, R.; Martens, J. A.; Mullens, S.; Maurer, F. H. J.; Vankelecom, I. F. J. *J. Membr. Sci.* **2006**, *278*, 83.

(6) Duval, J. M.; Folkers, B.; Mulder, M. H. V.; Desgrandchamps, G.; Smolders, C. A. *J. Membr. Sci.* **1993**, *80*, 189.

(7) Vankelecom, I. F. J.; De Kinderen, J.; Dewitte, B. M.; Uytterhoeven, J. B. *J. Phys. Chem. B* **1997**, *101*, 5182.

(8) Vankelecom, I. F. J.; De Beukelaer, S.; Uytterhoeven, J. B. *J. Phys. Chem. B* **1997**, *101*, 5186.

(9) Gevers, L. E. M.; Aldea, S.; Vankelecom, I. F. J.; Jacobs, P. A. *J. Membr. Sci.* **2006**, *281*, 741.

(10) Gevers, L. E. M.; Vankelecom, I. F. J.; Jacobs, P. A. *J. Membr. Sci.* **2006**, *278*, 199.

(11) Aerts, P.; Kuypers, S.; Genné, I.; Leysen, R.; Mewis, J.; Vankelecom, I. F. J.; Jacobs, P. A. *J. Phys. Chem. B* **2006**, *110*, 7425.

(12) Zhang, Y.; Li, H.; Lin, J.; Li, R.; Liang, X. *Desalination* **2006**, *192*, 198.

(13) Avramescu, M. E.; Borneman, Z.; Wessling, M. *Biotechnol. Bioeng.* **2003**, *84*, 564.

(14) Mulder, M. *Basic Principles of Membrane Technology*; Kluwer Academic Publishers: Dordrecht, 1996.

membranes to benefit from the incorporation of fillers in the separating layer, it is clear that the fillers need nanoscale dimensions in order to avoid defects. In this respect, the recently developed silicalite-1 nanozeolites¹⁶ seem very attractive. These are in fact the building blocks from which conventional silicalite zeolites are constructed and which can be isolated under specific conditions.

This paper presents the first incorporation of these nano-sized zeolites in polymeric membranes. During the investigations, cloudy mixtures were repeatedly found when adding suspensions of these nanozeolites to polymer casting solutions. Instead of observing the expected inorganic aggregates or precipitated polymer pieces, these turbid mixtures turned out to be stable emulsions. The solidification of these emulsions via phase inversion resulted in membranes with micron-sized pores, for which the emulsion droplets acted as templates, and whose pore walls are covered with nanozeolites. Moreover, dense defect-free skin layers able to discriminate on a molecular level could be prepared thanks to the introduction of a short evaporation step prior to coagulation of the polymer film to selectively reduce the pore size at the film surface. As these observations obviously opened interesting prospects for the preparation of a new class of organomineral membranes, but also more general polymeric materials with controlled porosity, the creation of these emulsions and their transformation into solid polymers were studied in more detail. Two typical applications, namely in solvent resistant nanofiltration (SRNF)¹⁷ and in controlled drug release,¹⁸ will also be presented to prove the practical viability of the presented method. Finally, the benefits of the new method will shortly be compared to the commonly used methods to prepare porous solids. The new synthesis method will be referred to as solidification of emulsified polymer solutions via phase inversion (SEMPI).

2. Experimental Section

2.1. Preparation of Silicalite-1 Nanozeolite Suspensions. An aqueous nanozeolite suspension containing silicalite-1 precursor species was prepared according to a procedure described by Ravishankar et al.¹⁶ Twenty-five grams of tetraethylorthosilicate (TEOS, Acros, 98%) was slowly added to 18 g of a concentrated, aqueous tetrapropylammonium (TPA) hydroxide solution (Alfa, 40% in water) under gentle stirring. After clarification of the turbid mixture, the resulting aqueous suspension (AS) was further stirred overnight. In contrast to the literature procedure, no extra water was added here. Subsequently, 40 g of AS was added to 80 g of a 1 M HCl (Acros, 37% in water) solution in *N*-methyl-2-pyrrolidone (NMP, Acros, 99.5%). Ethanol and water were selectively removed by a 1 h treatment in a rotating vaporizer at 80 °C and 50 mbar. The obtained acidified, NMP-based nanoparticle suspension,

hereafter denominated as NMP-S, was stored at 4 °C to inhibit further condensation of the species. A similar solvent exchange procedure was followed to transfer the nanozeolites to other polymer-compatible solvents, i.e., *N,N*-dimethylformamide (DMF, Acros, 99.8%) and *N,N*-dimethylacetamide (DMAc, Acros, 99.8%), thus obtaining the corresponding DMF- and DMAc-based nanozeolite suspensions (DMF-S and DMAc-S).

2.2. Characterization of Silicalite-1 Nanozeolite Suspensions.

The remaining water in NMP-S was determined using an Aquacounter AQV300 volumetric Karl Fisher moisture titrator (JM Science), while the solid content was found through gravimetric analysis after evaporation of the solvent at 100 °C under vacuum. The solids recovered after evaporation were calcined at 450 °C (36 h) to remove the TPACl present in the nanozeolite pores, thus allowing determination of the silica content of the nanozeolite suspension.

Dynamic light scattering (DLS) measurements were performed on a noninvasive backscattering (NIBS) high performance particle sizer (ALV), equipped with a photomultiplier detector. The samples were pretreated using a filter with a pore size of 200 nm. Particle sizes were corrected for the suspension viscosities, determined with an automated microviscosimeter (Anton Paar).

2.3. Preparation of Casting Solutions.

Casting solutions (total weight 18 g) were synthesized by mixing a solvent (NMP, DMF, or DMAc) with the corresponding nanozeolite suspension (NMP-S, DMF-S, or DMAc-S), followed by the addition of polymer and finally tetrahydrofuran (THF, Acros, 99.5%) as volatile cosolvent. This way, ternary/quaternary polyimide (PI, Matrimid 9725 US, Huntsman), polysulfone (PSf, Udel P-1835, Solvay), polyethersulfone (PES, Radel A, Solvay), polyphenylsulfone (PPhSf, Radel R, Solvay), and polyvinylidene fluoride (PVDF, Solef 6010/1001H, Solvay) solutions were prepared. For polycaprolactone (PCL, PolySciences), 1,4-dioxane (Acros, 99.5%) was used as solvent. All solutions were stirred magnetically until complete dissolution of the polymer.

TPACl (Janssen Chimica, 98%) and silica (Hi-Sil 233D, PPG Industries) were used to simulate NMP-S.

In the case of surfactant-based PI solutions, sorbitan trioleate (Span 85, Uniqema; HLB-value 2), sorbitan monostearate (Span 60, Uniqema; HLB 5), sorbitan monolaurate (Span 20, Uniqema; HLB 9), cetyltrimethylammonium bromide (CTAB, Acros; HLB 10), polyoxyethylene (20) sorbitan trioleate (Tween 85, Uniqema; HLB 11), polyoxyethylene (20) sorbitan monooleate (Tween 80, Uniqema; HLB 15), and sodium dodecyl sulfate (SDS, Fluka; HLB 40) were used. A certain amount of surfactant and water were added to a NMP/THF mixture, to which PI was finally added.

2.4. Characterization of Emulsified Polymer Solutions.

Optical imaging of polymeric emulsions was carried out on a Jenaval microscope using a Kodak DC40 digital camera. Morphology and elemental composition of an emulsified PSf casting solution was studied by cryogenic scanning electron microscopy (cryo-SEM) using a Philips XL30 FEG scanning electron microscope equipped with an Emitech K1250 cryogen preparation system and an energy dispersive X-ray (EDX) microanalysis system. After freezing a drop of the polymer solution under liquid nitrogen, the sample was sublimated (−90 °C, 20 min), sputter-coated (40 mA, 2 min) with an ultrathin Au layer, and transferred to the SEM chamber (−156 °C) under vacuum.

Macroscopic phase separation of a PSf-based emulsion was obtained through centrifugation (15 000 rpm, 15 min), after which the composition of both phases was determined gravimetrically via gradual heat treatment at 100 °C (6 h) and 450 °C (36 h).

2.5. Membrane Preparation.

Integrally skinned asymmetric membranes were prepared via immersion-precipitation. The

- (15) Vankelecom, I. F. J.; De Smet, K.; Gevers, L. E. M.; Jacobs, P. A. In: Schäfer, A. I.; Fane, A. G.; Waite, T. D. (Eds.) *Nanofiltration—Principles and Applications*; Elsevier: Amsterdam, 2004; pp 33–65.
- (16) Ravishankar, R.; Kirschhock, C. E. A.; Knops-Gerrits, P. P.; Feijen, E. J. P.; Grobet, P. J.; Vanoppen, P.; De Schryver, F. C.; Mieke, G.; Fuess, H.; Schoeman, B. J.; Jacobs, B. A.; Martens, J. A. *J. Phys. Chem. B* **1999**, *103*, 4960.
- (17) Vandezande, P.; Gevers, L. E. M.; Vankelecom, I. F. J. *Chem. Soc. Rev.* **2008**, *37*, 365.
- (18) Dinh, S. M.; Liu, S. M. *Advances in Controlled Drug Delivery: Science, Technology and Products*; ACS Symposium Series; American Chemical Society: Washington, DC, 2003.

homogeneous polymer solutions were cast (1.2 m/min) on a polyethylene/polypropylene nonwoven fabric (Viledon FO2471, Freudenberg) attached to a stainless steel plate using an automatic film applicator (Braive Instruments). In order to allow partial evaporation of the volatile THF, the nascent polymer films with a wet-film thickness of 250 μm were exposed for 30 s to ambient air at 20 ± 1 °C and $50 \pm 5\%$ relative humidity. The cast films were then immersed in deionized water at 20 °C, after which the membranes were air-dried at room temperature.

2.6. Membrane characterization. Membrane morphology was examined with SEM using a Philips XL30 FEG scanning electron microscope, i.e. a semi-in-lens type microscope with a cold field-emission electron source. Cross-sections were obtained by breaking the membranes under liquid nitrogen. All samples were coated with an ultrathin Pt/Pd coating using a Cressington HR208 high-resolution sputter coater (1 min, 20 mA), thus reducing sample charging under the electron beam.

The performance of PI membranes in SRNF was assessed through filtration experiments at room temperature. Circular coupons were cut from the membrane sheets and mounted in a laboratory-made stainless steel dead-end pressure cell (membrane surface area 15.2 cm^2). Pure 2-propanol (IPA) and a 250 $\mu\text{mol/L}$ solution of the dye Rose Bengal (RB, Fluka; 1017 g/mol) in IPA were used as typical SRNF feeds. In all cases, 50 mL of feed solution was poured into the cell, which was stirred at 700 rpm and subsequently pressurized to 20 bar with nitrogen gas. Permeate samples were collected in cooled flasks as a function of time, weighed to determine permeances ($\text{L m}^{-2} \text{h}^{-1} \text{bar}^{-1}$) and analyzed. Rejections (%) are defined as $(1 - C_p/C_f) \times 100$, where C_f and C_p denote the solute concentrations in the initial feed and in the permeates, respectively. Dye concentrations were measured on a Perkin-Elmer lambda 12 UV-vis spectrophotometer at 558 nm. All filtrations were performed in duplicate; average performances are reported.

2.7. Drug Release Test. A solution containing 18 wt % PSf, 1 wt % of the drug metoprolol (Sigma, 99+%), 25 wt % NMP-S, and 56 wt % NMP was solidified via precipitation from the vapor phase in an atmosphere at 75% relative humidity. To remove all NMP, the polymer film was immersed in acetone for 24 h, prior to starting a typical in vitro release study in deionized water. Release rates were assayed using an isocratic HPLC method at room temperature. The HPLC system (Merck Hitachi LaChrom) consisted of a L-7100 pump, a L-7200 autosampler equipped with a 100 μl loop, a L-7240 UV detector set at 260 nm, and an interface D-7000. Metoprolol analysis was performed on a LiChrospher RP sel. B 5 μm (dimensions 125 \times 4 mm) column (Knauer).

3. Results and Discussion

3.1. Characterization of the Nanozeolite Suspension.

For the initial aqueous nanozeolite suspension (AS), the maximum of the particle size distribution curve, measured by DLS, is situated around a dynamic diameter of 1.9 nm (Figure 1), with an important “shoulder” at lower diameters. As expected from the synthesis conditions of AS, involving no addition of extra water, this value is smaller than the dynamic diameter of 2.8 nm¹⁶ reported in literature for the so-called “nanoslabs”,^{16,19,20} slab-shaped silicalite-1 intermediates with dimensions of 1.3 \times 4.0 \times 4.0 nm³. This observation implies that the prepared suspension basically

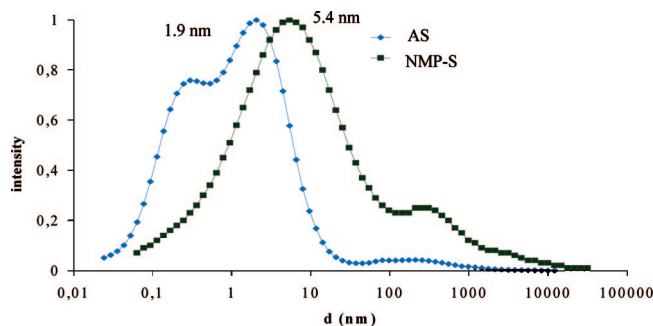


Figure 1. Evolution of the particle size distribution of the aqueous nanozeolite suspension (AS) upon solvent exchange (NMP-S), as obtained with DLS (normalized signals).

consists of nanoslab precursors ($1.3 \times 1.3 \times 1.0 \text{ nm}^3$),²⁰ and their oligomers.

Ethanol and water, respectively formed in the hydrolysis of TEOS and the condensation of silanols, are both nonsolvents for most common polymers to which the nanozeolite suspension should be added. This obviously impedes the use of the synthesized AS as additive for polymer solutions, thus necessitating further treatment. As dry isolation of the zeolite precursors is not possible without their aggregation into micron-sized particles, a solvent exchange procedure was established, as described here for NMP. First, the AS was added to an acidified NMP solution, after which water and ethanol were selectively evaporated at 80 °C under vacuum, thus generating a NMP-based nanozeolite suspension (NMP-S). The acidification was carried out to avoid polymer degradation upon addition of the highly basic AS to polymer solutions. As a consequence, also the charge-neutralizing mantle of physisorbed TPA⁺ cations at the surfaces of the precursor species was replaced by protons. Due to the solvent exchange and heat treatment, an increase of the maximal particle diameter to 5.4 nm was observed for NMP-S (Figure 1). As aggregation of the precursors seems implausible because of the low water content of the mixture, this relatively large value is expected to be an overestimation in DLS. It can possibly be ascribed to strong hydrogen bonding between the silanol groups on the surface of the species and the NMP solvent molecules acting as Lewis bases, thus restricting the mobility of the precursors. This way, a stabilizing NMP-mantle is formed around the nanozeolite species. This would also explain the week-long stability of NMP-S when refrigerated.

Gravimetric analysis of NMP-S revealed the presence of 8 ± 1 wt % nanosized zeolites, an equal amount of TPACl, and less than 3 wt % of water. TPACl is present due to the reaction of the TPA⁺ cations at the surface of the zeolitic species with HCl, added upon solvent exchange. Similar nanoparticle loads were found for nanozeolite suspensions prepared in other aprotic solvents (DMF-S and DMac-S). With this modified synthesis procedure, polymer-compatible suspensions of nanozeolites in organic solvents were formed, allowing straightforward addition to casting solutions. As the nanodimensions of the species were preserved, defect-free membrane synthesis via phase inversion was anticipated (see section 3.6.1).

3.2. Addition of Nanozeolite Suspensions to Polymer Solutions and Their Influence on Membrane Morphology.

(19) Kirschhock, C. E. A.; Ravishankar, R.; Verspeurt, F.; Grobet, P. J.; Jacobs, P. A.; Martens, J. A. *J. Phys. Chem. B* **1999**, *103*, 4965.

(20) Kirschhock, C. E. A.; Ravishankar, R.; Van; Looveren, L.; Jacobs, P. A.; Martens, J. A. *J. Phys. Chem. B* **1999**, *103*, 4972.

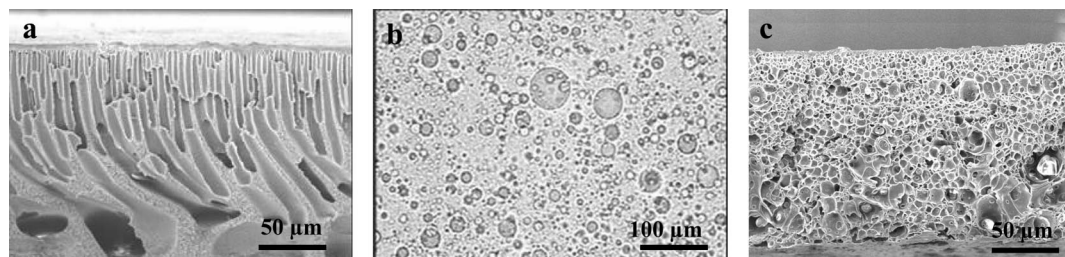


Figure 2. (a) SEM image of the cross-section of an unfilled PI membrane, (b) light microscopy image of an emulsified PI solution and (c) the corresponding membrane structure.

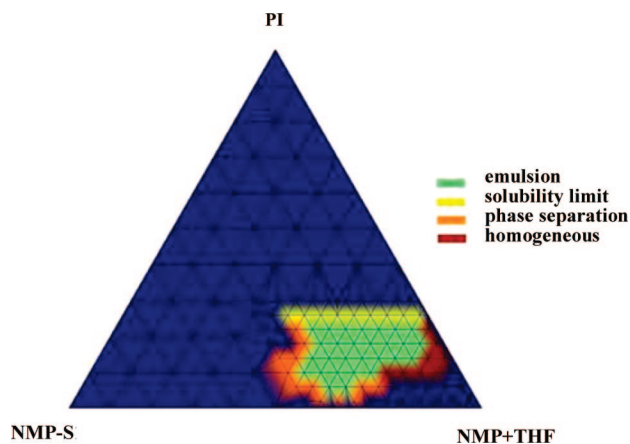


Figure 3. Compositional diagram showing the area in which stable emulsions can be formed in PI solutions (fixed THF/NMP weight ratio of 1/3). All axes scaled from 0 to 100 wt %.

3.2.1. Generation of Polymeric Emulsions and Transformation into Membranes. Solidification of polymer solutions to turn them into membranes, is usually achieved through phase inversion of a cast polymer film by immersion in a water bath. Such production of porous membranes is—under the conditions applied here—typically associated with the development of macrovoid-rich^{14,15} polymer structures (Figure 2a). Most unexpectedly, cloudiness was observed in a PI solution as soon as a certain amount of NMP-S was added. Observations with an optical microscope did not reveal the presence of undissolved species or aggregates but proved, on the other hand, the existence of droplets. Surprisingly, the casting solution was thus in fact transformed into an emulsion (Figure 2b). Moreover, all emulsions were stable for at least a month. The membranes cast from such emulsions clearly showed a spongelike structure (Figure 2c), with the spherical micron-sized pores apparently originating from the original emulsion droplets. This most interesting membrane structure in particular, obtained under conditions that would normally favor macrovoid formation, and the as-such surprising formation of polymeric emulsions, in general, initiated the following more in-depth investigation.

3.2.2. Compositional Boundaries for Emulsion Formation. Emulsification was clearly dependent on the amount of NMP-S added to the casting solution. For PI solutions at constant THF/NMP solvent weight ratio, the compositional boundaries within which stable emulsions could be formed can be represented in a ternary diagram, as shown in Figure 3. The emulsification area is set by the solubility limit of PI at ca. 26 wt %, the macroscopic phase separation at high solvent concentrations, and the formation of a monophasic

system at low NMP-S and/or low PI concentrations.

3.2.3. Versatility of Emulsion Formation. Quite surprisingly, stable emulsified polymer solutions (Figure 4 top) were also easily obtained with many other polymers, including PSf (Figure 4a), PES (Figure 4b), PPhSf, PVDF (Figure 4c), and PCL, thus proving the generality of the SEPPi method. Typical compositions of these casting solutions were as follows: 15 wt % PSf, 10 wt % DMF-S, 56.3 wt % DMF, 18.7 wt % THF; 15 wt % PES, 10 wt % NMP-S, 56.3 wt % NMP, 18.7 wt % THF; 15 wt % PPhSf, 10 wt % NMP-S, 56.3 wt % NMP, 18.7 wt % THF; 22.5 wt % PVDF, 10 wt % DMAc-S, 50.6 wt % DMAc, 16.9 wt % THF; and 15 wt % PCL, 15 wt % NMP-S, 70 wt % 1,4-dioxane. After casting and solidification via immersion—precipitation in water, all these polymeric emulsions resulted in spongelike membrane structures (Figure 4 bottom), reflecting the original emulsion morphology into the final pores. In order to explain the observed morphologies, the next step was to try to understand the role of the inorganic additive in this process.

3.3. Role of the Nanozeolite Suspension in the Formation and Stabilization of Polymeric Emulsions. In order to facilitate discrimination of the different phases in elemental analysis, a sulfur-containing polymer was chosen for this investigation. An emulsified PSf solution with elevated nanozeolite concentration for easy Si detection was thus investigated with cryo-SEM and EDX microanalysis (Figure 5). The emulsion droplets are clearly enriched with silicon, oxygen, and chlorine, originating from the added zeolite precursor solution. The continuous phase containing the polymer, on the other hand, is enriched in carbon and sulfur. Macroscopic phase separation of this PSf emulsion via simple centrifugation, followed by gravimetric determination of the composition of both phases through gradual heat treatment, also indicated the presence of a polymer-rich continuous phase and a polymer-poor dispersed phase, with the nanoparticles mainly present in the latter phase (Table 1). These observations indicate that the nanosized particles act as alternatives to surfactants or block copolymers to stabilize and control emulsions, which is reminiscent of the so-called particle stabilized “Pickering” emulsions.^{21–25} Besides the stabilization of emulsion droplets with colloidal particles, another stabilization mechanism might play. The steady viscosity increase of PI solutions noticed upon adding NMP-S suggests an increased polymer concentration in the continuous phase and hence a decreased droplet mobility. With the addition of extra liquid to a casting solution leading to an increased overall viscosity, a “solvent transfer” from the continuous to the dispersed phase can be presumed, in

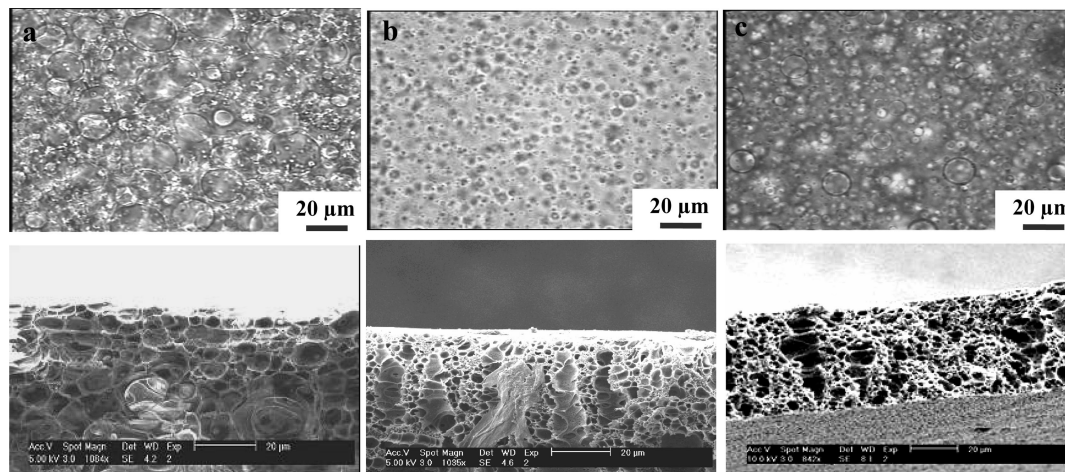


Figure 4. SEPMI method illustrated for (a) PSf, (b) PES, and (c) PVDF. Top: Light microscopy images of polymeric emulsions. Bottom: SEM images of the cross-sections of the corresponding membranes. See section 3.2.3 for the compositions of the polymer solutions.

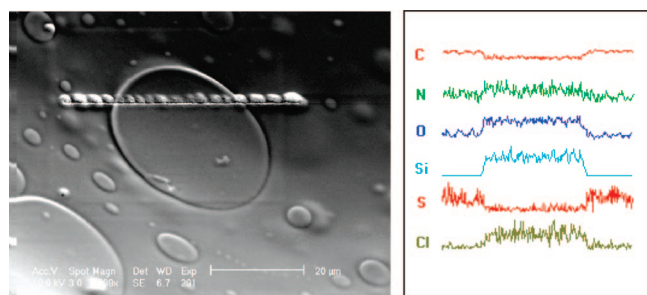


Figure 5. Cryo-SEM image of emulsified PSf solution (18 wt % PSf, 47.5 wt % NMP-S, 34.5 wt % NMP), with an indication of a line scan, and the corresponding elemental EDX microanalysis.

Table 1. Composition of Centrifugation-Separated Phases of Emulsified PSf Solution,^a Analyzed Gravimetrically via Gradual Heat Treatment

	composition (wt %)	
	continuous phase	dispersed phase
NMP + THF + H ₂ O	78.1	83.6
PSf + TPACl	20.3	3.5
Si	1.6	12.9

^a 18 wt % PSf, 32.5 wt % NMP-S, 37.1 wt % NMP, 12.4 wt % THF.

line with the cryo-SEM microanalysis results (Figure 5) and the compositional analysis of the phases (Table 1). Together, these two stabilization mechanisms hinder coalescence of the droplets and further growth of the dispersed phase, thus explaining the observed long-term stability of the emulsions with unchanged droplet sizes over several weeks.

Apart from its stabilizing effect on the formed droplets, the emulsion-inducing effect of the nanozeolite suspension is evidently crucial as well. The most probable hypothesis explaining the formation of stable emulsions is a destabilization of the casting solution by the constituents of the nanozeolite additive. To investigate this, PI solutions with different polymer concentrations and different NMP-S concentrations were titrated with deionized water until macroscopic phase separation was visually observed. The compositions of the polymeric emulsions at the onset of phase separation are indicated in Figure 6. For mixtures with increasing NMP-S concentrations, less water is clearly needed for phase separation, thus confirming the destabilizing effect of the additive. The zeolite precursor solution can thus

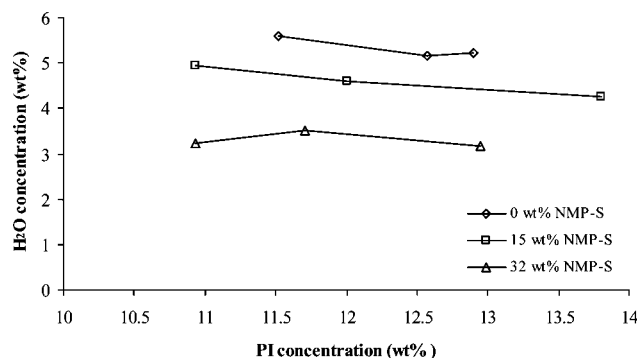


Figure 6. Composition of PI solutions (THF/NMP weight ratio of 1/3) at the onset of macroscopic phase separation upon titration with water.

be considered as a nonsolvent additive,^{26,27} destabilizing the continuous polymer phase and assisting in the solidification process. On the level of the membrane, this nonsolvent character manifests itself in the disappearance of macrovoids^{28,29} upon addition of NMP-S (Figure 2).

Subsequently, it was investigated which component exactly in the complex NMP-S mixture (see section 3.1) induced these effects. In the first instance, the effect of water, generally a strong nonsolvent additive for polymeric solutions, was studied. Upon addition of 4 wt % water to a 15 wt % PI solution, a membrane with a bicontinuous pore network structure was obtained, clearly different from the well-defined spherical pores in the SEPMI membranes. The formation of this network structure can be ascribed to

(21) Aveyard, R.; Binks, B. P.; Clint, J. H. *Adv. Colloid Interface Sci.* **2003**, *100*, 503.
 (22) Stratford, K.; Adhikari, R.; Pagonabarraga, I.; Desplat, J.; Cates, M. *Science* **2005**, *309*, 2198.
 (23) Clegg, P. S.; Herzig, E. M.; Schofield, A. B.; Horozov, T. S.; Binks, B. P.; Cates, M. E.; Poon, W. C. K. *J. Phys.: Condens. Matter* **2005**, *17*, S3433.
 (24) Vermant, J.; Ciocco, G.; Nair, K. G.; Moldenaers, P. *Rheol. Acta* **2004**, *43*, 529.
 (25) Chung, H. J.; Taubert, A.; Deshmukh, R. D.; Composto, R. J. *Europhys. Lett.* **2004**, *68*, 219.
 (26) Kim, I. C.; Lee, K. H.; Tak, T. M. *J. Membr. Sci.* **2001**, *183*, 235.
 (27) Lai, J. Y.; Lin, F. C.; Wang, C. C. *J. Membr. Sci.* **1996**, *118*, 49.
 (28) McKelvey, S. A.; Koros, W. J. *J. Membr. Sci.* **1996**, *112*, 29.
 (29) Smolders, C. A.; Reuvers, A. J.; Boom, R. M.; Wienk, I. M. *J. Membr. Sci.* **1992**, *73*, 259.

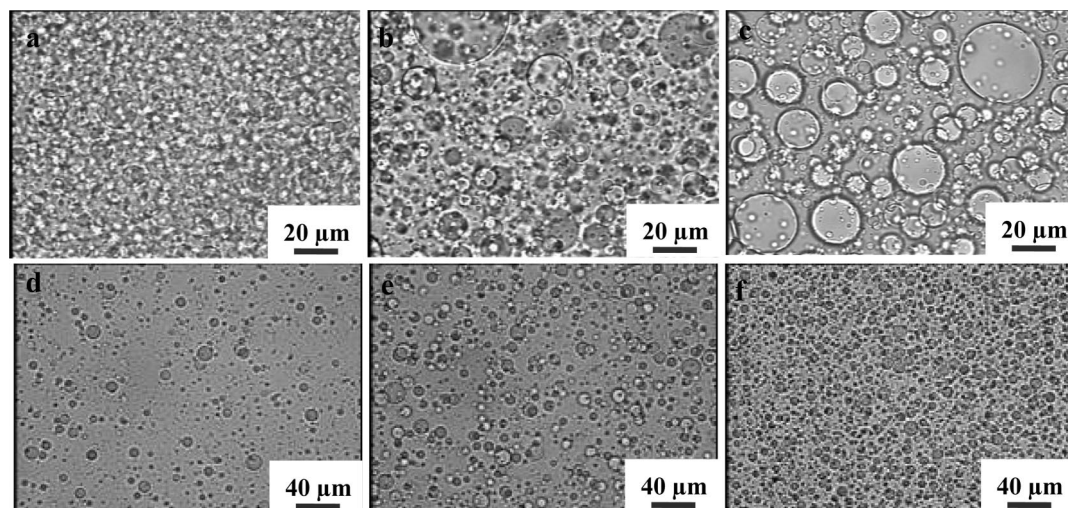


Figure 7. Top: Emulsion morphology of PSf solutions with NMP-S concentrations of (a) 32.5 wt %, (b) 42.5 wt %, and (c) 47.5 wt % (12 wt % PSf, THF/NMP weight ratio of 1/3). Bottom: Emulsion morphology of PSf solution (18 wt % PSf, 22.5 wt % NMP-S, THF/NMP weight ratio of 1/3) subjected to (d) magnetic stirring and (e) high shear mixing at 250 rpm and (f) 2000 rpm.

spinodal decomposition^{30,31} in the polymer solution upon coagulation. In a next step, in order to elucidate to what extent the nanosized particles themselves are responsible for the observed morphologies, PI/NMP/THF mixtures were prepared with only TPACl and water added, in the same concentrations as present in NMP-S (see section 3.1). SEM analysis revealed a decrease in the number of macrovoids as compared to an unfilled reference membrane. However, a clear sponge structure was not observed, and no droplets could be discerned in the casting solution. The NMP suspension was also simulated with a mixture of TPACl, water, and precipitated silica, all in the same concentration as in NMP-S. In this case, a macrovoid-containing membrane structure was formed, very similar to an unfilled reference membrane (Figure 2a), and again no emulsification was achieved in the polymer solution. These observations thus indicate that none of the individual constituents of NMP-S, nor a limited combination of them, brings about the same membrane morphology as obtained through addition of the complete additive. The presence of the surface-active nanosized zeolites is thus indispensable for emulsification of polymer solutions and for the membrane morphologies ensuing from it.

Given the theoretical model of the silicalite-1 nanoslab structure reported in literature,^{16,19} an external zeolite surface of 1227 m² per gram can be calculated, on which in total 5.6×10^{21} silanol groups are present. The presence of this enormous number of silanol groups, protonated under the acid (pH < 2) conditions of NMP-S, might explain the destabilizing effect of the zeolite precursors on polymer solutions. The huge specific surface area obviously also allows interactions with the polymer chains in the continuous phase, thus contributing to the stability of the emulsions and the final porous materials.

3.4. Manipulation of Droplet Size. With droplets in the emulsions directly linked to pores in the solidified material,

easy tuning of the droplets would enable facile pore manipulation in the solid state as well. Possible manipulation of droplet size and number was first investigated by increasing the NMP-S concentration in PSf solutions. As shown in Figure 7a–c, a significant increase of the droplet size is induced. Because of the nonsolvent character of NMP-S (see section 3.3.), liquid–liquid demixing becomes more prominent at higher concentrations, and more droplets are formed. The higher number of droplets, in turn, favors Ostwald ripening and coalescence and might thus explain the observed increase in droplet size.

A second very simple way to tune the droplet size was found in the mechanical agitation of the polymer solutions. The use of a high-shear mixer (Figure 7e,f) instead of a magnetic stirrer (Figure 7d) allows a more homogeneous droplet size distribution and a decreased droplet size. The shear exerted by the mixer artificially increases the contact area between the polymer chains and the solvent mixture, which is understandably small for these systems due to the nonsolvent properties of the nanozeolite additive. This causes destabilization and demixing of the polymer solution, resulting in a more pronounced droplet formation.

3.5. Extension of SEPPI to Surfactants. The possibility to emulsify polymer solutions through the addition of conventional surfactants was investigated, since the extension to other surface-active compounds would make the SEPPI method even more versatile. Droplet formation—as observed through optical microscopy—could be induced by the combined addition of some water and surfactant. In contrast to polymer solutions emulsified through the addition of NMP-S, these emulsions were not visually turbid. The screening involved a selection of surfactants with hydrophilic/lipophilic balances (HLB) ranging from 2 to 40 (Table 2). Addition of charged surfactants resulted in macroscopically phase-separated systems, possibly due to the pronounced nonsolvent power of such surfactants. Only surfactants with intermediate HLB values, like Tween 85 and Span 20, in combination with some water, achieved emulsification in PI solutions. The concentration of the added water and surfactant in the final polymer solution was crucial. Addition of at

(30) Van de Witte, P.; Dijkstra, P. J.; van den Berg, J. W. A.; Feijen, J. J. *Membr. Sci.* **1996**, *117*, 1.

(31) Wienk, I. M.; Boom, R. M.; Beerlage, M. A. M.; Bulte, A. M. W.; Smolders, C. A.; Strathmann, A. H. R. *J. Membr. Sci.* **1996**, *113*, 361.

Table 2. Use of Surfactants in the Preparation of Emulsified PI Solutions^a

surfactant	HLB value	charge	stability ^b	emulsion ^c
Span 85	2	0	+	—
Span 60	5	0	+	—
Span 20	8.6	0	+	+
CTAB	10	+	—	—
Tween 85	11	0	+	+
Tween 80	15	0	+	—
SDS	40	+	+	—

^a 15 wt % PI, 4 wt % H₂O, 4 wt % surfactant. ^b Stability: (+) thermodynamically stable system or (—) system with complete phase separation, thus not allowing membrane formation ^c Emulsion: (+) formation of an emulsion or (—) a homogeneous solution.

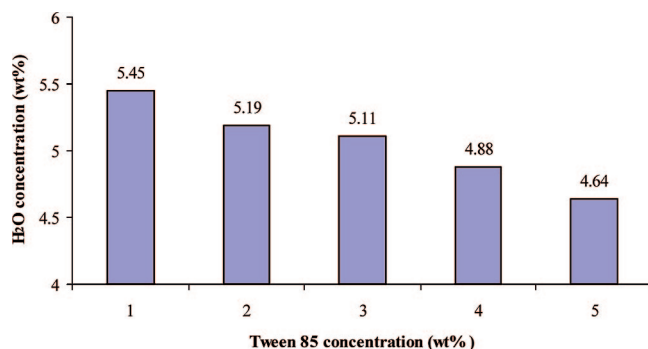


Figure 8. Composition of PI solutions (15 wt % PI, THF/NMP weight ratio of 1/4) containing Tween 85 surfactant at the onset of macroscopic phase separation upon titration with water.

least 4 wt % water was needed to induce emulsion formation, irrespective of the amount and type of surfactant added, while polymer solutions with 5 wt % water were stable emulsions at lower surfactant concentrations only. The upper limit for the water concentration in the mixture, determined through titration with water until macroscopic phase separation, was highly dependent on the surfactant concentration (Figure 8). Despite the smaller compositional area for emulsification as compared to polymer/nanozeolite systems, the observations with surfactants extend the versatility of the presented SEPMI method (Figure 9).

3.6. Practical Utility of the SEPMI Concept. *3.6.1. Performance of PI-Based SEPMI Membranes in SRNF.* By introducing a short evaporation step prior to immersing cast SEPMI-based polymer films in a nonsolvent bath,¹⁵ asymmetric SRNF membranes with dense, defect-free skin layers could be prepared. The volatile cosolvent THF, evaporating from the cast film, locally creates an elevated polymer concentration at the membrane surface. The THF concentration in the casting solution and the evaporation time thus offer easy control over the density of the selective membrane skin layer.

Comparison of a SEPMI membrane, cast from a THF/NMP (weight ratio of 1/2) solution containing 18 wt % PI and 18 wt % NMP-S, with the commercially available, also PI-based, Starmem 120 membrane showed that a 4-fold IPA permeance (20 bar, room temperature) increase could be achieved at the expense of only a relatively small decrease in RB rejection from 99.8 to 98.0% at equilibrium. A reference, unfilled PI membrane with the same polymer concentration showed a 96.6% rejection and an intermediate equilibrium flux. Highly permeable membranes, often result-

ing from high porosity structures, are more susceptible to compaction, resulting in an important time-dependent reduction of the membrane flux, especially at high pressures. Figure 10 shows a pure IPA flux reduction of only 26% for the SEPMI membrane. This flux reduction is comparable to that of the Starmem membrane, which has a much lower equilibrium permeance. The flux of the reference membrane is initially also high, but it is more than halved in less than 1 h. The absence of compaction-sensitive macrovoids in SEPMI membranes, their typical spongelike appearance, and the presence of incompressible inorganic particles contribute to this superior mechanical stability. The elevated fluxes also confirm the presence of an interconnected pore network throughout the SEPMI polymer matrix.

3.6.2. SEPMI Polymers as Controlled Release Agents. Porous polymers are known as attractive controlled release agents.¹⁸ The SEPMI approach, allows to manipulate pore structure and skin layer density, and thus offers easy tools to readily tailor release rates. For biological applications, biocompatible polymers like PSf and biodegradable polymers like PCL can be used. As the drug molecules can be added during the preparation already, a postsynthesis loading of the drugs, often resulting in low yields, can be avoided. High encapsulation efficiencies up to 50 wt % of the model drug metoprolol could be realized with a 18 wt % emulsified PSf solution. With emulsion solidification taking place upon immersion in water, part of the water-soluble, incorporated drug might leach out during the formation of the release agent. However, low-polarity alcohols, like hexanol, could still induce phase inversion while significantly reducing drug leaching. In order to completely prevent drug leaching, dry phase inversion via precipitation from the vapor phase^{14,15} was applied instead of the usual immersion-precipitation. In a 75% relative humidity atmosphere, solidification took place already after a few seconds. To remove all NMP, the membrane was immersed in acetone, a nonsolvent for the drug but well-miscible with NMP, prior to starting a typical in vitro release study in deionized water. About 1.5% of the total amount of loaded metoprolol was released after 60 h at room temperature from a particular polymer composition, containing 1 wt % drug incorporated in a 250 μm thick PSf film, cast from an NMP solution containing 18 wt % PSf and 25 wt % NMP-S.

3.7. Comparison of SEPMI with Existing Methods to Prepare Porous Polymers. Porous polymers shaped as films, monoliths or particles have widespread applications, e.g. in chromatography,³² filtrations,¹⁴ electronics,³³ sensors,³⁴ (bio)-catalysis,³⁵ cell culture applications,³⁶ controlled release,³⁷

(32) Eeltink, S.; Decrop, W. M. C.; Rozing, G. P.; Schoenmakers, P. J.; Kok, W. K. *J. Sep. Sci.* **2004**, *27*, 1431.

(33) Zhang, Y.; Zha, S.; Liu, M. *Adv. Mater.* **2005**, *17*, 487.

(34) Lin, V. S. Y.; Motesharei, K.; Dancil, K. S.; Dailor, M. J.; Ghadiri, M. R. *Science* **1997**, *278*, 840.

(35) McNamara, C. A.; Dixon, M. J.; Bradley, M. *Chem. Rev.* **2002**, *102*, 3275.

(36) Richardson, T. P.; Peters, M. C.; Ennett, A. B.; Mooney, D. J. *Nat. Biotechnol.* **2001**, *19*, 1029.

(37) Sant, S.; Nadeau, S.; Hildgen, P. *J. Controlled Release* **2005**, *107*, 203.

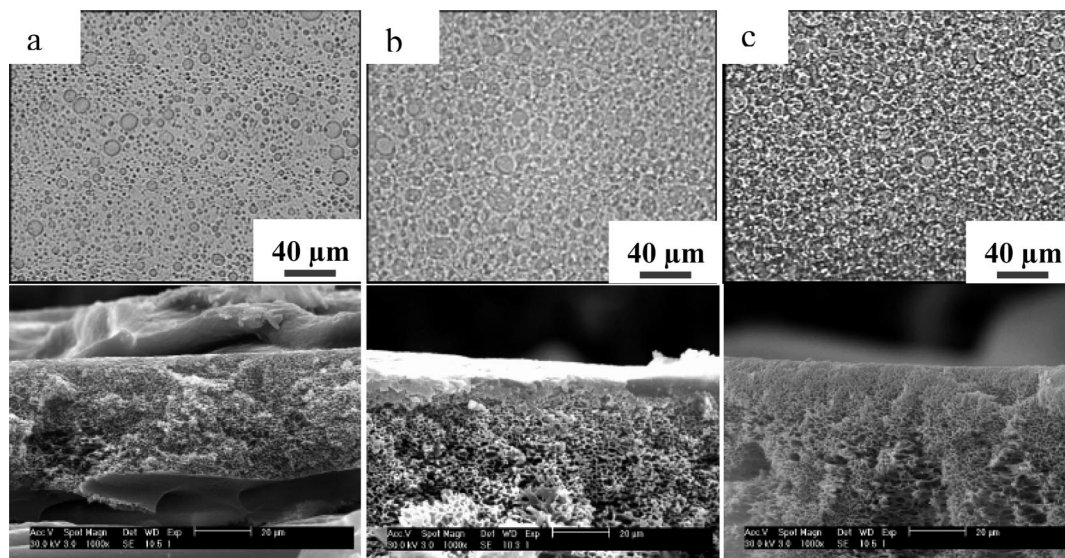


Figure 9. Top: Morphology of Tween 85-stabilized PI emulsions (15 wt % PI, THF/NMP weight ratio of 1/4): (a) 2 wt % Tween 85, 5.19 wt % H₂O; (b) 3 wt % Tween 85, 5.11 wt % H₂O; and (c) 5 wt % Tween 85, 4.64 wt % H₂O. Bottom: SEM images of the cross sections of the corresponding membranes.

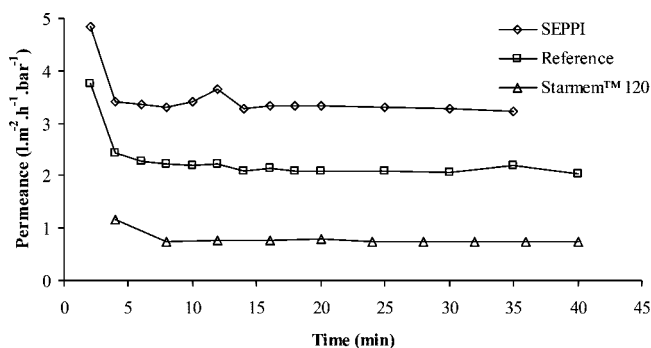


Figure 10. Pure IPA permeance (20 bar, room temperature) through PI-based SEPPi membrane (18 wt % PI, 18 wt % NMP-S, THF/NMP weight ratio of 1/2), reference PI-membrane (idem without NMP-S), and Starmem™ 120.

tissue engineering scaffolds,³⁸ and gene therapy.³⁹ The most common methods to create porous polymers are phase inversion,¹⁴ foaming,^{40,41} gas blowing,⁴² and the use of liquid porogens,⁴³ supercritical fluids,⁴⁴ or templates.⁴⁵ So-called templating methods generate porosity either via self-assembly techniques^{46,47} and molecular imprinting⁴⁸ or via the use of

colloids^{49,50} or emulsions^{51,52} as templates for the pores. After solidification of the polymer through electron irradiation⁵³ or UV curing,⁵⁴ the template is removed via solvent extraction or thermal decomposition. Template methods tend to be particularly time-consuming and difficult to scale up.⁵⁵ In emulsion templating methods, most closely related to SEPPi, the continuous phase of an emulsion, initially consisting of monomers or macromonomers, solidifies upon polymerization. A particular case of emulsion templating leads to polyHIPEs, prepared by the polymerization of high-internal-phase emulsions (HIPEs).⁵⁶ Hydrophobic porous polymers can thus be obtained by polymerization of the continuous phase of water-in-oil type emulsions, typically containing styrene monomer and divinylbenzene cross-linker,⁵⁷ while hydrophilic monomers such as acrylamide^{58–60} polymerize in the continuous aqueous phase of an oil-in-water emulsion. The use of monomers with intermediate hydrophobicity is difficult due to emulsion instability.⁶⁰ Generally, large fractions of expensive surfactants are required to stabilize HIPEs effectively, but titania nanoparticles have been used as well, resulting in polyHIPEs with improved properties.⁶¹ Functionalized porous polyHIPE membranes⁶² with a thickness of around 100 μm have been reported recently for the fabrication of electrochemical

(38) Salem, A. K.; Rose, F. R. A. J.; Oreffo, R. O. C.; Yang, X.; Davies, M. C.; Mitchell, J. R.; Roberts, C. J.; Stolnik-Trenkic, S.; Tendler, S. J. B.; Williams, P. M.; Shakesheff, K. M. *Adv. Mater.* **2003**, *15*, 210.
 (39) Saltzmann, W. A. *Nat. Biotechnol.* **1999**, *17*, 534.
 (40) Barbetta, A.; Dentini, M.; DeVecchis, M. S.; Fillipini, P.; Formisano, G.; Caiazza, S. *Adv. Funct. Mater.* **2005**, *15*, 118.
 (41) Siripurapu, S.; DeSimeone, J. M.; Khan, S. A.; Spontak, R. J. *Adv. Mater.* **2004**, *16*, 989.
 (42) Li, Q.; Matuana, L. M. *J. Appl. Polym. Sci.* **2003**, *88*, 3139.
 (43) Dong, Y. S.; Guo, C.; Lin, P. H.; Yin, L. H.; Pun, Y. P. *Key Eng. Mater.* **2005**, *381*, 288–289.
 (44) Cooper, A. I. *Adv. Mater.* **2003**, *15*, 1049.
 (45) Xia, Y.; Gates, B.; Yin, Y.; Lu, Y. *Adv. Mater.* **2000**, *12*, 693.
 (46) Stenzel-Rosenbaum, M. H.; Davis, T. P.; Fane, A. G.; Chen, V. *Angew. Chem., Int. Ed.* **2001**, *40*, 3428.
 (47) Srinivasarao, M.; Collings, D.; Philips, A.; Patel, S. *Science* **2001**, *292*, 79.
 (48) Schmidt, R. H.; Belmont, A.; Haupt, K. *Anal. Chim. Acta* **2005**, *542*, 118.

(49) Lu, C.; Qi, L.; Cong, H.; Wang, X.; Yang, J.; Yang, L.; Zhang, D.; Ma, J.; Cao, W. *Chem. Mater.* **2005**, *17*, 5218.
 (50) Velez, O. D.; Kaler, E. W. *Adv. Mater.* **2000**, *12*, 531.
 (51) Zhang, H.; Cooper, A. I. *Soft Matter* **2005**, *1*, 107.
 (52) Imhof, A.; Pine, D. J. *Nature* **1997**, *389*, 948.
 (53) Cho, S. O.; Jun, Y. J.; Ahn, K. A. *Adv. Mater.* **2005**, *17*, 120.
 (54) Schmidt, R. H.; Moschbach, K.; Haupt, K. *Adv. Mater.* **2004**, *15*, 719.
 (55) Yan, F.; Goedel, W. A. *Adv. Mater.* **2004**, *16*, 911.
 (56) Silverstein, M. S.; Tai, H.; Sergienko, A.; Lumelsky, Y.; Pavlovsky, S. *Polymer* **2005**, *46*, 6682.
 (57) Cameron, N. R.; Sherrington, D. C. *J. Mater. Chem.* **1997**, *7*, 2209.
 (58) Cameron, N. R. *Polymer* **2005**, *46*, 1439.
 (59) Krajnc, P.; Stefanec, D. *12th International Conference on Polymers and Organic Chemistry*; Okazaki, Japan, 2006.
 (60) Butler, R.; Davies, C. M.; Cooper, A. I. *Adv. Mater.* **2001**, *13*, 1459.
 (61) Menner, A.; Ikem, V.; Salgueiro, M.; Shaffer, M. S. P.; Bismarck, A. *Chem. Commun.* **2007**, *41*, 4274.
 (62) Ruckenstein, E. *Adv. Polym. Sci.* **1997**, *127*, 1.

sensors.⁶³ PolyHIPE materials have been used as membrane films for the removal of particulates from aerosols⁶⁴ and as ion exchange resins⁶⁵ but also as chromatographic supports,⁶⁶ supports for solid-phase chemistry,⁶⁷ matrices for cell culture,⁶⁸ and scaffolds for tissue engineering.⁶⁹ In contrast to other emulsion templating methods, SEPPI does not involve a chemical reaction for the solidification of the polymer but a simple physical phase inversion. The need of controlled reaction atmospheres and risks of side reactions can thus be eliminated, while this also renders the method applicable to a wider range of polymers.

Conclusions

A novel versatile route to prepare polymers with controlled porosity is presented here, involving the preparation of an emulsion of controlled morphology in a polymer solution, followed by its subsequent solidification by simple contact with a nonsolvent for the polymer. The presented SEPPI method allows the creation of porous materials from a wide variety of polymers with easily tunable pore size, thanks to the presence of droplets in the polymer solutions, resulting

from the presence of nanosized zeolites or surfactants. The emulsified polymers can be easily solidified upon simple contact with nonsolvents or their vapors, with the droplets in the emulsion acting as template for the spherical pores in the final films. These micron-sized spherical pores are in turn connected with each other via smaller pores in the polymer matrix.

The method is easy, practical and flexible, allows creation of anisotropic structures, and does not involve any chemical reaction in the solidification process nor tedious template extraction or decomposition procedures. Furthermore, the presence of the droplets in the polymer solutions and the effect of the nanoparticles also hand extra parameters to morphology control. Insertion of an evaporation step prior to immersion in the nonsolvent bath enables the synthesis of selective, asymmetric, high-flux SEPPI membranes with a high compaction resistance. Room temperature drug loading at high concentrations can be combined with reaction-free support solidification, without drug leaching during preparation. The abundant presence of functional groups at the pore walls, created without any polymer postsynthesis derivatization, could also open new opportunities in, for example, chromatography, sensors, and catalysis.

Acknowledgment. P.V. and L.E.M.G. acknowledge Katholieke Universiteit Leuven and IWT Flanders, respectively, for a grant as doctoral research fellows. This research was done in the frame of a IAP project on Functional Supramolecular Systems sponsored by the Belgian Federal Government, of a GOA project funded by the Flemish Government, and of the Centre of Excellence in Catalytic Science (CECAT).

CM800231N

-
- (63) Zhao, C.; Danish, E.; Cameron, N. R.; Katakya, R. *J. Mater. Chem.* **2007**, *17*, 2446.
(64) Akay, G.; Bhumgara, Z.; Wakeman, R. J. *Chem. Eng. Res. Des.* **1995**, *73*, 782.
(65) Wakeman, R. J.; Bhumgara, Z. G.; Akay, G. *Chem. Eng. J.* **1998**, *70*, 133.
(66) Krajnc, P.; Leber, N.; Stefanec, D.; Kontrec, S.; Podgornik, A. *J. Chromatogr. A* **2005**, *1065*, 69.
(67) Cetinkaya, S.; Khosravi, E.; Thompson, R. *J. Mol. Catal. A: Chem.* **2006**, *254*, 138.
(68) Baker, S. C.; Atkin, N.; Gunning, P. A.; Granville, N.; Wilson, K.; Wilson, D.; Southgate, J. *Biomaterials* **2006**, *27*, 3136.
(69) Busby, W.; Cameron, N. R.; Jahoda, C. A. B. *Polym. Int.* **2002**, *51*, 871.